



Biosorption of crystal violet onto cyperus rotundus in batch system: kinetic and equilibrium modeling

Bharathi Kandaswamy Suyamboo, Ramesh Srikrishnaperumal*

*Department of Civil Engineering, National Institute of Technology, Tiruchirappalli 620 015, Tamil Nadu, India
Tel. +91 431 250 3166; Fax: +91 431 250 0133; email: stramesh@nitt.edu*

Received 6 December 2011; Accepted 23 April 2013

ABSTRACT

In this study, biosorption potential of *Cyperus rotundus* (CR) was investigated for decolorization of crystal violet (CV), a cationic dye, from its aqueous solution employing batch experimental set-up. Experiments were carried out as a function of contact time, biosorbent dosage (0.1–2.0 g), initial solution pH (2–12), temperature (20–40 °C), initial dye concentration (10–30 mg/l), and agitation speed (50–200 rpm). The biosorbent (before and after dye biosorption) was characterized by Fourier transform infra red spectroscopy and scanning electron microscopy. The Langmuir, Freundlich, and Temkin adsorption isotherm models were used for the mathematical description of biosorption equilibrium. The biosorption process followed the Freundlich isotherm model with high correlation coefficient at different temperatures. The pseudo-second-order kinetic model fitted well in correlation to the experimental results. The mass transfer model based on intraparticle diffusion was applied to the experimental data to examine the mechanisms of the rate controlling step. It was found that intraparticle diffusion was not the sole rate controlling step. Thermodynamic parameters, such as ΔG , ΔH , and ΔS were also calculated for the biosorption process and found that the biosorption process is spontaneous and exothermic in nature. It can be concluded that CR is a promising biosorbent for the removal of CV from aqueous solution.

Keywords: Biosorption; *Cyperus rotundus*; Crystal violet; Equilibrium; Kinetics; Thermodynamics

1. Introduction

The introduction of waste products into the environment is an important problem that has been highlighted by various environmentalists [1]. Industrial effluents are one of the major causes of environmental pollution because effluents discharged from dyeing industries are highly colored with a large amount of suspended organic solid [2]. The colored wastewater

not only influence the aesthetic acceptability of the receiving waters, but also influence aquatic life by hindering light penetration and disturbing the food chain organisms leading to ecological imbalance [3]. Dyes can also cause allergic dermatitis and skin irritation [4]. Many dyes are difficult to decolorize due to their complex aromatic molecular structure and synthetic origin, [5–10] which provide them physico-chemical, thermal, and optical stability [11]. Hence, it is imperative that a suitable treatment method should be devised [12]. Techniques such as coagulation, chemical

*Corresponding author.

precipitation, membrane filtration, electrochemical degradation, reverse osmosis, photo catalytic degradation, solar photo-Fenton and biological processes, and adsorption have been tested and evaluation for the treatment of dye bearing effluents [13]. In particular, the use of agricultural waste in adsorption system has been drawn attention from a large number of researchers because: (i) it is abundantly available; (ii) most of the types of agriculture waste are readily to be used and do not require a complex pretreatment step or activation process before application; (iii) regeneration of these adsorbents may not be necessary (unlike activated carbon, where regeneration is essential); and (iv) less maintenance and supervision are required for the operation of the adsorption process [14]. A number of non-conventional, low-cost adsorbents, such as maize cob [15], palm kernel fibre [16], rice hush [17], ground nut shell [18], orange peel [19], lemon peel [20], rice bran [21], and wheat bran [21] have been used to remove dyes from wastewater. The advantage of using these waste materials is that it saves disposal costs while alleviating potential environmental problems. *Cyperus rotundus* (CR) (coco-grass, purple nut sedge, red nut sedge) is a species of sedge (Cyperaceae) native to Africa and Southern Asia. It is a perennial plant that may reach a height of up to 55 inches. CR is one of the most invasive weeds known having spread out to a worldwide distortion in tropical and temperate regions. It has been called the world's worst weed. Despite that many low-cost adsorbents have been studied for decontamination purposes, studies on the CR as an economical biosorbent for dye removal have not entered the scientific literature. The aim of the present study was to investigate the dye biosorption potential of CR for Crystal Violet (CV) removal from aqueous solutions in batch system. The study includes an evaluation of the effects of various operational parameters, such as contact time, biosorbent dosage, pH, temperature, initial dye concentration, and agitation speed on the dye biosorption process. The adsorption kinetic models, equilibrium isotherm models, and thermodynamics parameters related with this process were also performed and reported.

2.1. Preparation and characterization of biosorbent

CR were collected from the local farmlands in Tiruchirappalli, Tamil Nadu, India. It was first thoroughly washed with tap water to remove dust, dirt, and any unwanted particles. The biosorbent was then sundried and subsequently oven dried at 60°C for 24 h. The dried biomass were ground to fine powder using a grinder and sieved to a constant size

(150–300 µm) and used as biosorbent without any pretreatment for CV biosorption.

Textural characterization of the prepared biosorbent was carried out by Quanta chrome NOVA 2200C USA, surface area analyzer. A gas mixture of 22.9 mol% nitrogen and 77.1 mol% helium was used for this purpose. The Brunauer, Emmett, Teller (BET) surface area was then determined. Fourier transform infrared ((FTIR - 2000, Perkin-Elmer) analysis was done on the unused biosorbed and the dye loaded biosorbent to determine the surface functional groups that might be involved in CV biosorption. The biosorbent was encapsulated in a KBr disk and by pressing the ground material with 8MT pressure bench press, the translucent disks were obtained. The FTIR spectrum was recorded in the wave number range 4,000–400 cm⁻¹ at 4 cm⁻¹ spectral resolution. In addition, the surface structure of the biosorbent, before and after biosorption was analyzed by a Scanning Electron Microscope (HITACHI S-3000H) at an electron acceleration voltage of 25 kV. Prior to scanning, the unloaded and dye-loaded CR samples were mounted on a stainless steel stab with double stick tape and coated with a thin layer of gold in high vacuum condition.

2.2. Evaluation of zero point charge (pH_{zpc})

A series of 50 mL of 0.01 M NaCl solution was placed in a closed Erlenmeyer flask. The pH was adjusted to a value between 2.0 and 12.0 by adding 0.1 M HCl or 0.1 M NaOH solution. Then 50 mg of each CR sample was added and agitated at 150 rpm for 2 h under atmospheric conditions. The final pH was measured and the results were plotted with ΔpH (initial pH–final pH) against final pH. The pH_{zpc} is the point where the curve pH_{final} vs. pH_{initial} crosses the line pH_{initial} = pH_{final} [22].

2.3. Preparation of adsorbate solutions

CV used in this study was of commercial quality (CI 42555 MF: C₂₅ H₃₀ Cl N₃, λ_{max} = 579 nm) and used without further purification. Dye stock solution (1,000 mg/l) was prepared by dissolving accurately weighed quantity of the dye in double distilled water. Experimental dye solution of different concentrations was prepared by diluting the stock solution with suitable volume of double distilled water.

2.4. Batch biosorption studies

Batch biosorption experiments were carried out in 250 mL Erlenmeyer flasks with 50 mL of working

volume, with a concentration of 10 mg/l. A weighed amount (50 mg) of biosorbent was added to the solution. The flasks were agitated at a constant speed of 150 rpm for 3 h in an orbital shaker (IHC-3280) at 30°C. The influence of contact time biosorbent dosage (0.1–2.0 g/L), pH (2.0–12.0), initial dye concentration (10–30 mg/l), temperature (20–40°C), and agitation speed (50–200 rpm) were evaluated in the present study. Samples were collected from the flasks at pre-determined time intervals and the supernatant solution was separated from the CR by centrifugation at 10,000 rpm for 5 min. The residual amount of dye in each flask was determined using UV/VIS spectrophotometer (Lambda 25). The amount of dye adsorbed per unit CR (mg dye per g biosorbent) was calculated according to a mass balance on the dye concentration using Eq. (1):

$$q_e = \frac{(C_o - C_e)V}{m} \quad (1)$$

where C_o is the initial concentration of the dye (mg/l), C_e is the equilibrium dye concentration in solution (mg/l), V is the volume of the solution (L) and m is the mass of the biosorbent. The percent removal (%) of dye was calculated using the following equation:

$$\text{Removal (\%)} = \frac{C_o - C_e}{C_o} \times 100 \quad (2)$$

3. Theory

3.1. Biosorption isotherms

In the analysis and design of a biosorption process, isotherms provide the most important information in understanding the biosorption process [23]. The equation parameters and the underlying thermodynamic assumption of the isotherm models give some idea about the underlying biosorption mechanism as well as the surface properties and affinity of the biosorbent [24]. Therefore, in the present study the biosorption equilibrium data were analyzed using Langmuir, Freundlich, and Temkin isotherm models. Linear regression is commonly used to determine the best-fitting isotherm and the applicability of isotherm equations is compared by judging the correlation coefficients, R^2 .

Langmuir model is based on the assumption that adsorption energy is constant and independent of surface coverage where the adsorption occurs on localized sites with no interaction between adsorbate molecules. The maximum adsorption occurs when the surface is covered by a monolayer of adsorbate. The linearized form of the Langmuir equation is expressed as:

$$\frac{1}{q_e} = \frac{1}{q_{\max}} + \frac{1}{q_{\max}b} \frac{1}{C_e} \quad (3)$$

where q_e (mg/g) and C_e (mg/l) are the amount of dye adsorbed, adsorbate per unit weight of adsorbent, and unadsorbed adsorbate concentration in solution at equilibrium, respectively. The constant b (l/g) is the Langmuir equilibrium constant and b/q_{\max} gives the theoretical monolayer saturation capacity. A plot of C_e/q_e vs. C_e gives a straight line of slope q_{\max}/b and intercepts $1/b$.

The essential characteristics of Langmuir equation can be expressed in terms of dimensionless separation factor, R_L defined by [25]:

$$R_L = \frac{1}{1 + K_L + C_o} \quad (4)$$

The R_L value implies whether the adsorption is unfavorable ($R_L > 1$), linear ($R_L = 1$), favorable ($0 < R_L < 1$), or irreversible ($R_L = 0$).

$$\log q_e = \log K + \frac{1}{n} \times \log C \quad (5)$$

where K (L/g) is the Freundlich constant and $1/n$ (g/l) is the heterogeneity factors, which are related to the capacity and intensity of the biosorption, respectively. A plot of $\log q_e$ vs. $\log C$ gives a straight line graph with $1/n$ as the slope and $\log K$ as the intercept.

The linear form of the Temkin equation is expressed as:

$$q_e = B_T(\ln A_T + \ln C_e) \quad (6)$$

where $B_T = R_T/b$, T is the absolute temperature in K, R the universal gas constant, 8.314 J/mol/K, A_T the equilibrium binding constant (l/mg), and B_T is related to the heat of adsorption. A plot of q_e vs. $\ln C_e$ enables the determination of the isotherm constants B_T and A_T from the slope and the intercept, respectively. A_T is the equilibrium binding constant (l/mg) corresponding to the maximum binding energy and constant B_T is related to heat of biosorption.

3.2. Kinetic modeling

The knowledge of the kinetics of any biosorption process is crucial in order to be able to design industrial scale separation processes [23]. Therefore, the data obtained from the contact time—temperature dependent experiments were used to study the kinetics of the biosorption process. The pseudo-first-order and pseudo-second-order kinetic models were tested

to obtain the rate constants and elucidate the underlying biosorption mechanism.

The linear form of the pseudo-first-order equation of Lagergren is generally expressed as [26].

$$\log(q_e - q_t) = \log(q_e) - \frac{k_1}{2.303}t \quad (7)$$

where q_e (mg/g) and q_t (mg/g) are the amount of adsorbate at equilibrium and at time t , respectively and k_1 (min^{-1}) is the rate constant of pseudo-first-order adsorption.

The pseudo-second-order chemisorptions kinetic equation is expressed as [26].

$$\left(\frac{t}{q_e}\right) = \frac{1}{k_2 q_e^2} + \frac{1}{q_e}t \quad (8)$$

where k_2 (g/mg min) is the equilibrium rate constant of pseudo-second-order adsorption. If the pseudo-second-order kinetic equation is applicable, the plot of t/q_t vs. t should give a linear relationship from which q_e and k_2 can be determined from the slope and intercept of the plot.

Since, the model mentioned above cannot identify a diffusion mechanism, the intra particle diffusion model was further used to determine the rate controlling step.

The intra particle diffusion equation is given as [27].

$$q_e = k_{td}t^{1/2} + C \quad (9)$$

When the intra particle diffusion alone is the rate limiting step, then the plot of q_t vs. $t^{1/2}$ passes through the origin. When film diffusion takes place, the intercept C gives the idea on the thickness of the boundary layer.

3.3. Thermodynamic studies

Thermodynamic parameters reflect the feasibility and spontaneous nature of the biosorption process. Thermodynamic behavior of biosorption of CV by CR was evaluated by the thermodynamic parameters—Gibbs free energy change (ΔG), enthalpy (ΔH), and entropy (ΔS). These parameters were calculated using the following equations:

$$K_o = \frac{C_{\text{solid}}}{C_{\text{liquid}}} \quad (10)$$

$$\Delta G = \Delta H - T\Delta S \quad (11)$$

$$\ln k_o = \frac{-\Delta G}{RT} \quad (12)$$

$$\ln k_o = \frac{-\Delta S}{R} - \frac{\Delta H}{RT} \quad (13)$$

where K_o is equilibrium constant, C_{solid} is solid phase concentration at equilibrium (mg/l), C_{liquid} is liquid phase concentration at equilibrium (mg/l), T is absolute temperature in Kelvin, and R is gas constant. ΔH and ΔS values can be obtained from the slope and intercept of plot $\ln K_o$ against $1/T$.

4. Results and discussion

4.1. Point of zero charge (pH_{zpc})

The point of zero charge (pH_{zpc}) or isoelectric point (pH_{IEP}) is an important factor that determines the linear range of pH sensitivity, and then indicates the type of surface active centers and the adsorption mobility of the surface [28]. From the result of pH_{zpc} measurement (figure not shown) the zero point charge of CR was found to be 5.6. The surface of the biosorbent will be negatively charged above pH_{zpc} and positively charged below pH_{zpc} [29]. There at a solution $\text{pH} > 5.6$, the CR process a negatively charged surface, which is favorable for biosorbing cationic CV.

4.2. Characterization of biosorbent

4.2.1. SEM analysis

In order to examine the surface morphology of the biosorbent, SEM micrographs were taken before and after CV biosorption and are presented in Fig. 1. Before dye uptake, the biosorbent is characterized by more fibrous material presenting some macro porous. The cavities of the fibrous materials were expanded, which should allow the diffusion of the dye molecule through the macro porous of the biosorbent. Following dye biosorption, pores are absent on the surface of CV loaded CR, suggesting the biosorption of CV onto CR. In addition, the appearance of a molecular cloud over the surface of dye-loaded biosorbent confirms the binding of dye ions to the functional group present in CR.

4.2.2. FTIR analysis

The FTIR spectral analysis is important to identify the different functional groups of the biosorbent surface which are responsible for biosorption of dye ions. The FTIR spectra of CR before biosorption and after

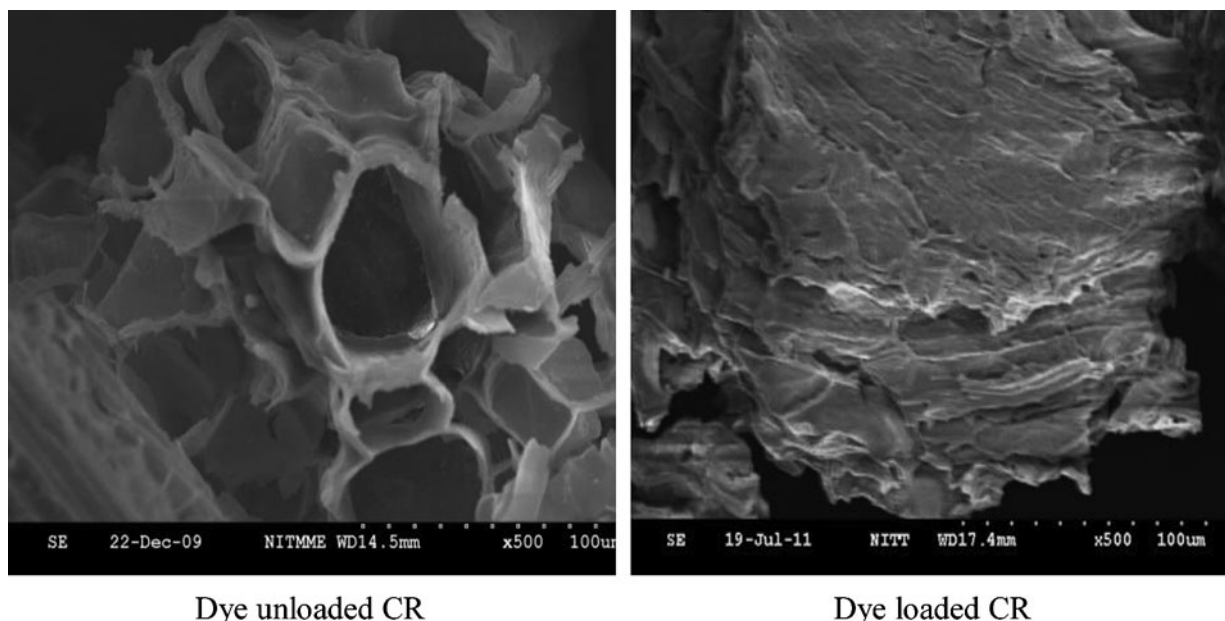


Fig. 1. SEM micrograph of CR before and after dye biosorption.

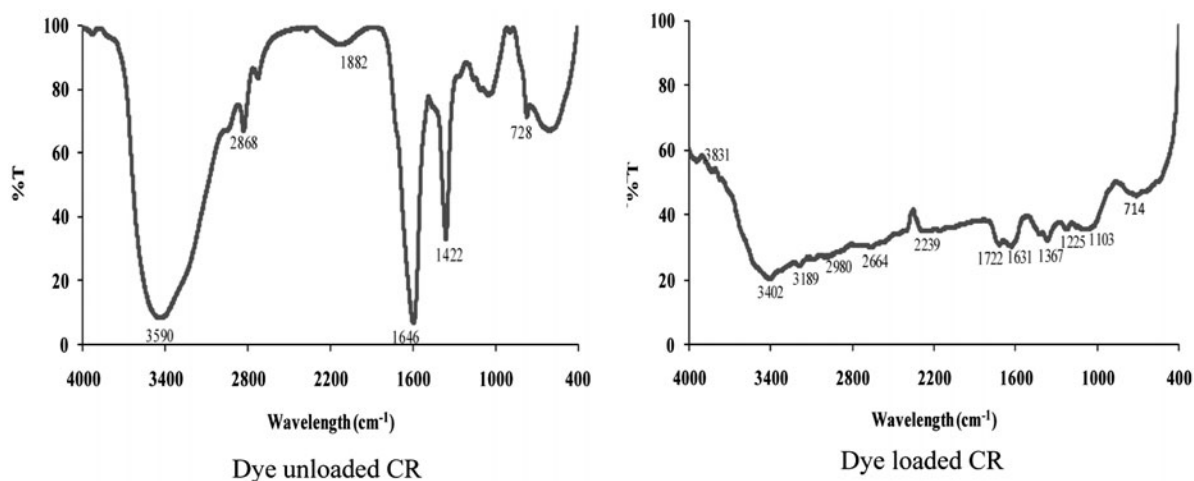


Fig. 2. FTIR spectrum of CR before and after dye biosorption.

biosorption of CV are shown in Fig. 2. The FTIR spectrum of CR (before biosorption) shows several distinct and sharp absorption peaks. The broad band at around $3,590\text{ cm}^{-1}$ represents bonded -OH groups [23]. The peak at $2,868\text{ cm}^{-1}$ is indicative of stretching of C-H bond of methyl and methylene groups [30]. The peak at $1,882\text{ cm}^{-1}$ can be attributed to unionized C=O stretching of carboxylic acid while the peak at $1,646\text{ cm}^{-1}$ is indicative of C=O stretching of carboxylic group with intermolecular hydrogen bond [30]. The peak at $1,422\text{ cm}^{-1}$ represents -C-O [31]. After biosorption of CV, the characteristic -OH bond at $3,590\text{ cm}^{-1}$ shift to

$3,831\text{ cm}^{-1}$. Also the peaks of unionized C=O stretching of carboxylic acid and that of C=O stretching of carboxylic group with intermolecular hydrogen bond shifts from $1,882$ and $1,646$ to $2,239$ and $1,722\text{ cm}^{-1}$, respectively. Thus, it can reasonably be said that -OH and -COOH groups can be the main binding sites for CV onto CR. The disappearance of the peak at $1,422\text{ cm}^{-1}$ (corresponding to -C-O) indicates that -C-O may be a potential sorption site in the CV biosorption process [23]. FTIR spectral analysis, thus, suggested the involvement of -OH , -C=O and -C-O functional groups in the biosorption of CV by CR.

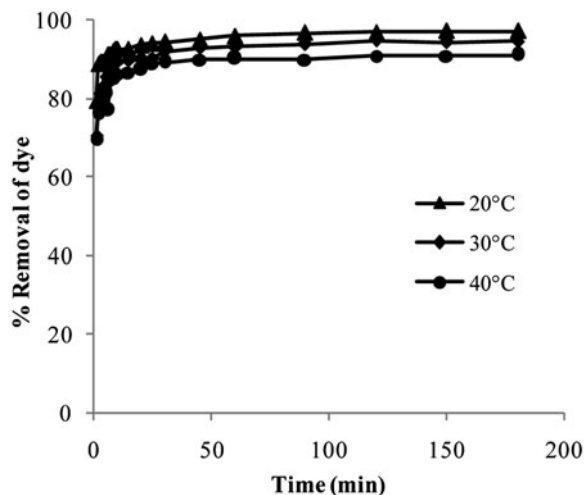


Fig. 3. Effect of contact time on biosorption of CV by CR ($C_0 = 10 \text{ mg/l}$; biosorbent dosage = 1 g/L ; particle size = $150\text{--}300 \mu\text{m}$; agitation speed = 150 rpm).

4.2.3. Textural characterization

The BET surface area of CR was found to be $1.013 \text{ m}^2/\text{g}$. The superficial area of agricultural residue is usually a low value [32,33].

4.3. Effect of contact time

The effect of contact time for the biosorption of CV by CR was studied and the results are shown in Fig. 3. As depicted in Fig. 3, it is clear that the dye was rapidly adsorbed in the first 45–60 min, and then the biosorption rate decreased gradually and reached equilibrium in about 120 min. This is due to the fact that, at the beginning, the biosorption rate was very fast as the dye ions were adsorbed by the exterior surface of CR. When the exterior surface of CR reached saturation, the dye ions entered into the pores of the biosorbent particles and were adsorbed by the interior surface of the solid particles. This process relatively takes a long time and the biosorption was slow [34].

4.3.1. Biosorption kinetics

The pseudo-first-order and pseudo-second-order kinetic models were used to obtain the rate constants and equilibrium biosorption capacity at different temperatures (Fig. 4(a) and (b)). The calculated model parameters along with the correlation coefficient values (R^2) are listed in Table 1. As can be seen from Table 1, the low R^2 (<0.90) values for the pseudo-first-order model indicate that this model was not suitable for describing the biosorption kinetics of CV onto CR.

However, the relatively high R^2 (>0.99) values for the pseudo-second-order model suggest that the ongoing

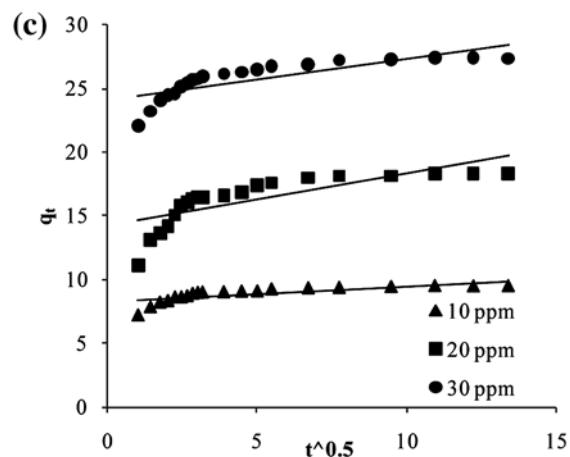
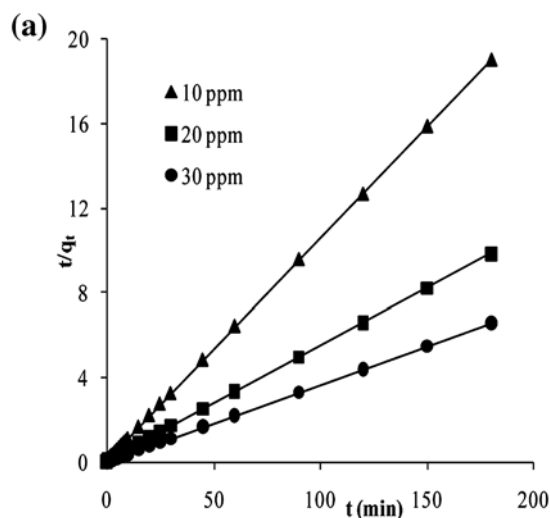
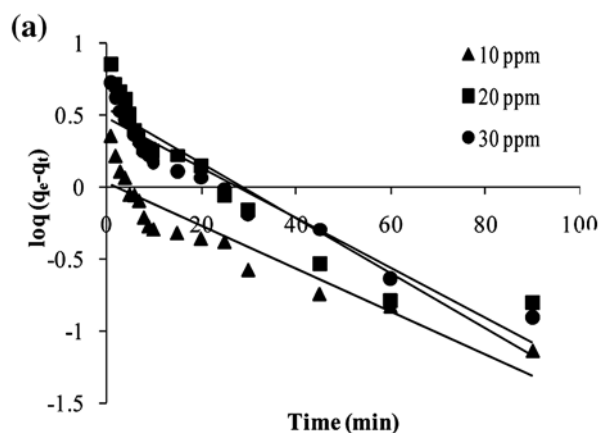


Fig. 4. Pseudo-first-order, pseudo-second-order and intraparticle diffusion plots for the biosorption of CV onto CR at different initial concentrations (particle size = $150\text{--}300 \mu\text{m}$; agitation speed = 150 rpm , temperature = 30°C).

Table 1
Adsorption kinetic model rate constants for CV removal

C_0	q_e (exp) (mg/g)	Pseudo-first-order-kinetic model			Pseudo-second-order kinetic model			Intra-particle diffusion model		
		q_e (cal) (mg/g)	k_1 (min^{-1})	R^2	q_e (cal) (mg/g)	k_2 (min^{-1})	R^2	K_{id} ($\text{mg/gmin}^{0.5}$)	C	R^2
10	9.50	1.06	0.032	0.85	9.52	0.167	1.00	0.317	24.11	0.65
20	18.22	3.548	0.044	0.87	18.51	0.05	0.99	0.406	14.19	0.61
30	27.37	2.985	0.039	0.92	27.77	0.065	1.00	0.122	8.229	0.59

biosorption process obeys pseudo-second-order kinetics at all studied temperatures. Also, as can be seen in Table 1, the calculated q_e values (q_e , cal) show good agreement with the experimental q_e values (q_e , exp), confirming that biosorption of CV onto CR follows the pseudo-second-order kinetic model. The applicability of the pseudo-second-order kinetic model indicates that the biosorption process of CV onto CR is chemisorptions and the rate-determining step is probably surface biosorption. The pseudo-second-order rate constant k_2 decreases with increase in temperature suggesting exothermic nature of the existing biosorption process.

In a well-agitated batch sorption system, there is a possibility of intraparticle pore diffusion of adsorbate ions, which can be the rate-limiting step. Therefore, the possibility of intra-particle diffusion resistance affecting the biosorption process was explored by using the intra-particle diffusion model (Eq. (9)). According to Eq. (9), a plot of q_t vs. $t^{0.5}$ should be a straight line, passing through the origin when the biosorption mechanism follows the intraparticle diffusion

process. However, if the data exhibit multi-linear plots, then the process is governed by two or more steps. The plots for biosorption of CV on CR at different temperatures were multimodal with three distinct regions (Fig. 4(c)). The initial curved region is attributed to the external surface biosorption in which the adsorbate diffuses through the solution to the external surface of the biosorbent. The second stage relates the gradual uptake reflecting intraparticle diffusion as the rate-limiting step. The final plateau region refers to the gradual biosorption stage and the final equilibrium stage, in which the intraparticle diffusion starts to slow down and level out. The present finding implies that although intraparticle diffusion is involved in the biosorption process, but it is not the sole rate-controlling step and that some other mechanisms also play an important role.

4.4. Effect of biosorbent dosage and temperature

Biosorbent dose is an important parameter that strongly influences the biosorption process by affecting biosorption capacity of the biosorbent [35]. Therefore, the influence of biosorbent dose on CV biosorption by CR was investigated in the range of 0.1–2.0 g. From Fig. 5, it is clear that the biosorption efficiency increased with an increase in biosorbent dosage. The increase in the percentage of dye removal with adsorbent dose could be attributed to an increase in the adsorbent surface area, augmenting the number of adsorption sites available for adsorption [35,36]. Further increase in adsorbent dose reduced the maximum removal of CV. The decrease in sorption capacity with increasing dose of adsorbent at constant dye concentration and volume may be attributed to saturation of adsorption sites due to particle interaction, such as aggregation [37]. Such aggregation would lead to a decrease in total surface area of the biosorbent and increase in diffusional path length [38]. The biosorption of CV by CR at different temperatures as a function of biosorbent dosage is shown in Fig. 6. The percentage

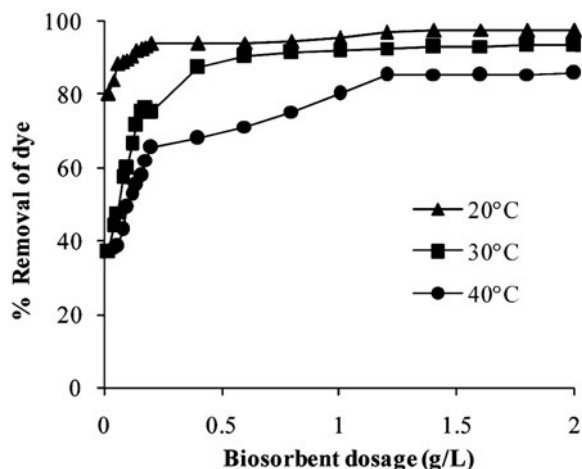


Fig. 5. Effect of biosorbent dosage on biosorption of CV by CR ($C_0=10$ mg/l; particle size = 150–300 μm ; agitation speed = 150 rpm).

removal of dye decreases slightly from 96.90 to 85.31% at the dose of 1.2 g/L when the solution temperature increases from 20 to 40 °C. This may be due to weakening of the bonds between the dye molecules and the binding sites of the biosorbent [39].

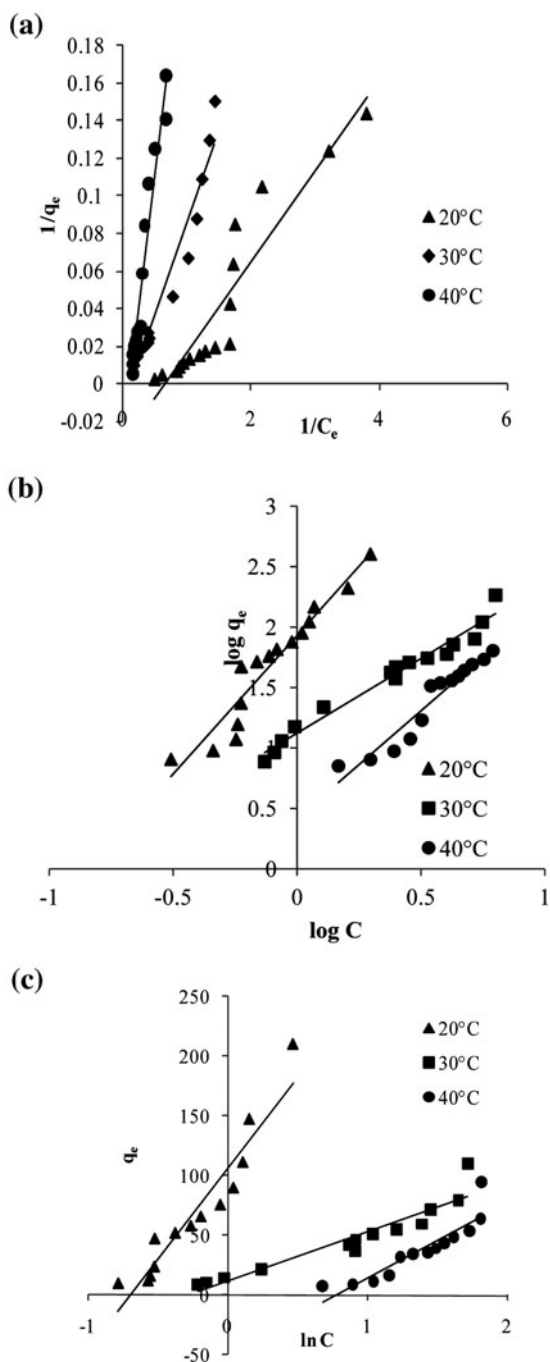


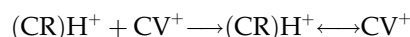
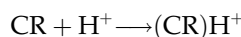
Fig. 6. Langmuir, Freundlich and Temkin isotherm plots for different temperatures on the biosorption of CV by CR ($C_0 = 10 \text{ mg/l}$; particle size = 150–300 μm ; agitation speed = 150 rpm).

4.4.1. Biosorption isotherms

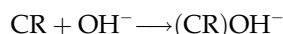
In the present investigation, the isotherm study for biosorption of CV by CR was conducted at different temperatures and the results are depicted in Fig. 6. The Langmuir, Freundlich, and Temkin isotherm models were used to describe the equilibrium biosorption data. The parameters obtained from the isotherm plots with the correlation coefficient are listed in Table 2. Analysis of the R^2 values suggests that the Freundlich isotherm model provides best fit to the equilibrium biosorption data than the other isotherm models at all studied temperatures. The maximum biosorption capacity decreased from 84.13 mg/g at 20 °C to 2.328 mg/g at 40 °C. These findings indicated an exothermic nature of the existing process.

4.5. Effect of pH

The effect of solution pH onto CV biosorption was studied in the pH range of 2.0–12.0. The result indicated that the maximum uptake of CV was found to be at pH 8.0 (Fig. 7). This behavior can be explained on the basis of change in the surface charge of CR. At lower pH, the H^+ ion concentration in the aqueous system increased and the surface of CR acquires positive charge by absorbing H^+ ions [34]. The positively charged surface sites on CR do not favor the biosorption of cationic dye due to the electrostatic repulsion, cause decrease in dye biosorption. As the pH of the aqueous system increases, the number of negatively charged sites increases by absorbing OH^- ions. As the CR surface gets negatively charged at high pH, a significantly high electro-static attraction exists between the negatively charged surface of CR and cationic dye molecules, leading to the maximum dye biosorption [34]. The following reactions were expected to occur at the solid/liquid interface:



(electrostatic interaction in basic medium)



(electrostatic interaction in basic medium)

Table 2
Biosorption isotherm constants for CV removal

Temperature (°C)	Langmuir isotherm constants			Freundlich isotherm constants			Temkin isotherm constants		
	q_{max} (mg/g)	b (L/mg)	R^2	K (mg/g)	n	R^2	A_T (L/mg)	B_T	R^2
20	-30.30	0.687	0.88	85.11	0.5	0.92	32.258	-0.064	0.77
30	-76.92	-0.132	0.948	13.27	0.74	0.97	90.90	0.545	0.709
40	-28.57	-0.121	0.946	2.61	0.51	0.93	35.714	0.714	0.772

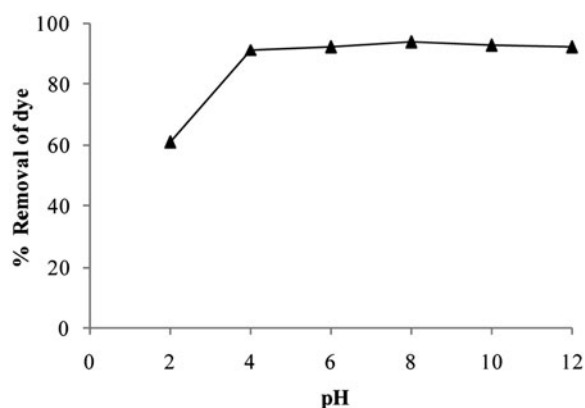


Fig. 7. Effect of pH on biosorption of CV onto CR ($C_0=10$ mg/l; particle size = 150–300 μ m; agitation speed = 150 rpm).

4.6. Effect of initial dye concentration

The effluent of different industries may have different dye concentrations. Initial dye concentration is one of the important factors that affect biosorption

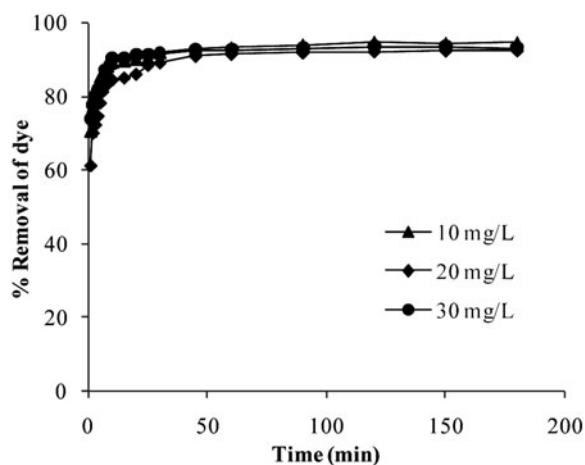


Fig. 8. Effect of initial concentration on biosorption of CV by CR (biosorbent dosage = 1 g/L; particle size = 150–300 μ m; agitation speed = 150 rpm; temperature = 30°C).

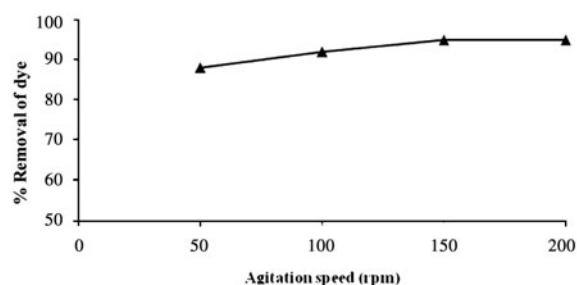


Fig. 9. Effect of agitation speed on biosorption of CV onto CR ($C_0=10$ mg/l; contact time = 180 min; temperature = 30°C; biosorbent dosage = 1 g/L).

kinetics. In order to study the effect of contact time and initial dye concentration on the CV uptake, 50 mL of CV solutions with initial concentration of 10, 20, and 30 mg/l were prepared in a series of 250 mL Erlenmeyer flasks. 50 mg of the biosorbent was added into each flask covered with glass stopper and the flasks were then placed in an isothermal water bath shaker at temperature of 30°C with rotation speed of 150 rpm, until equilibrium point was reached. In this case, the solution pH was kept original without any pH adjustment. Fig. 8 shows the effect of initial dye concentration of the CV uptake on the CLR and CR at 30°C. In the biosorption of CV by CR, it can be seen that percentage removal of dye decreases with increase in initial dye concentration. At lower

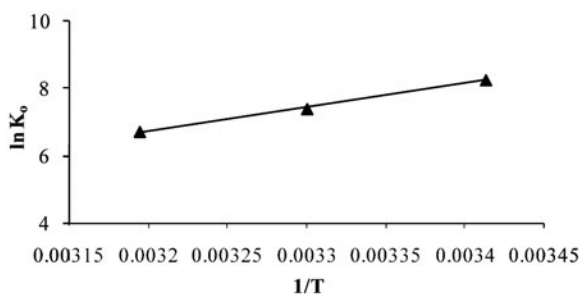


Fig. 10. Van't Hoff plot for effect of temperature on biosorption of CV onto CR.

Table 3
Thermodynamic parameters of CV over CR

Biosorbent	Initial CV concentration (mg/l)	ΔG (J/mole)			ΔH (J/mole)	ΔS (J/K/mole)
		293 K	303 K	313 K		
Cyperus rotundus	10	-20,087	-18,747	-17,405	-59,379	-134

Table 4
Comparison of CV biosorption capacity of CLR and CR with other reported low-cost sorbents

Sorbent	Maximum sorption capacity (mg/g)	References
Coir pith	2.56	[41]
Sugarcane dust	3.8	[42]
Neem sawdust	3.8	[43]
Calotropis procera leaf	4.14	[44]
Sagaun sawdust	4.25	[45]
Sugarcane fiber	10.44	[46]
Citrullus Lanatus rind	10.54	[47]
Orange peel	14.3	[48]
Wood apple	19.8	[49]
Jute fiber carbon	27.99	[50]
Coniferous pinus bark powder	32.78	[36]
Sawdust	37.83	[51]
Rice bran	42.25	[52]
Jackfruit leaf powder	43.39	[23]
Treated ginger waste	64.9	[34]
Wheat bran	80.37	[52]
Cyperus rotundus	85.11	This study

concentrations, all dye molecules present in the solution interact with the binding sites of the biosorbent, facilitating about 95% biosorption. However, all biosorbents have a limited number of binding sites, which become saturated at a certain concentration [14]. Hence, at higher concentrations, more dye molecules are left unadsorbed in the solution due to the saturation of binding sites resulting in decreased biosorption efficiency.

4.7. Effect of agitation on CV biosorption

It is well known that agitation is one of the important parameters governing an adsorption process, since it influences the distribution of the solute in the bulk solution and the formation of external boundary film [14]. The effect of agitation on the biosorption of CV by CR was studied at different agitation speeds

ranging from 50 to 200 rpm and the results are shown in Fig. 9. From Fig. 9 it was observed that the biosorption of CV by CR almost remained unchanged as agitation speed was increased. These observations can be explained by the fact that the boundary layer resistance was very small and the mobility of the system was high under experimental conditions [14]. In other words, the diffusion of the CV ion from the solution to the surface of the CR and into the pores occurred quickly and easily. Since the uptake of CV was not significantly influenced by the degree of agitation, an agitation speed of 150 rpm was, therefore, used for all further experiments.

4.8. Thermodynamic studies on biosorption of CV

Thermodynamic studies were performed to find the nature of the biosorption process. The values of ΔG were calculated using Eq. (11) and was found to be -20,087, -18,747, and -17,405 kJ mol⁻¹ at temperatures of 293, 303, and 313 K, respectively. The negative value of ΔG at different temperature indicated spontaneous nature of the biosorption process. ΔH and ΔS were determined from the slope and intercept of the plot $\ln K$ vs. $1/T$ (Fig. 10). In the biosorption of CV by CR, decrease in the negative value of ΔG with increasing temperature suggests that the biosorption process was more favorable at lower temperatures. The values of ΔH were calculated as -59,379 kJ/mol and -134 kJ/mol/K for ΔS (Table 3). The negative value of ΔH is indicative of the fact that the biosorption reaction was exothermic. The negative value of ΔS suggests that the process is enthalpy driven [40].

4.9. Comparison of various low-cost biosorbents

The maximum CV biosorption capacity of various sorbent materials including CR is summarized in Table 4. It is clear that CR has higher biosorption capacity of CV than many other reported sorbents. Differences in dye uptake capacity are differences in properties in of each sorbent material such as structure, functional groups and surface area [23]. The easy availability and cost effectiveness of CR are some

additional advantages, which makes it better biosorbent for the removal of CV from aqueous solution.

5. Conclusion

The percentage removal of the dye molecule decreased with increase in initial concentration and CV increased with decrease in temperature. The maximum biosorption was observed at pH 8.0. The FTIR analysis of CR showed that it can be used as a useful biosorbent for dye biosorption as it contains various functional groups on the surface. The Freundlich isotherm provided best fit to the experimental data indicating sorption on a heterogeneous surface. The maximum biosorption capacity was estimated to be 84.13 mg/g at 20°C. The biosorption kinetics followed pseudo-second-order kinetic model. Intra particle diffusion was not the sole rate controlling step. The negative value of ΔH indicated the process is exothermic. The negative value of ΔS suggests that the process is enthalpy driven. The maximum CV biosorption capacity of CR was comparable and found to be moderately higher than that of many corresponding sorbent materials under similar conditions. Results obtained from this study showed that the studied eco-friendly biosorbent, CR, could be used as an alternative potential biosorbent for the removal of CV from the aqueous solution in a static batch system. Since, the CR is freely, abundantly, and locally available, they can be put in use as economical sorbents for the treatment of effluent that accompanies the dyeing units and the dye stuff industries.

References

- E.L. Grabowska, G. Gryglewicz, Adsorption characteristics of Congo red on coal-based mesoporous activated carbon, *Dyes Pigm.* 74 (2007) 34–40.
- G. Crini, Nonconventional low cost adsorbents for dye removal: A review, *Bioresour. Technol.* 97(9) (2006) 1061–1085.
- S. Mona, A. Kaushik, C.P. Kaushik, Biosorption of reactive dye by waste biomass of *Nostoc linckia*, *Ecol. Eng.* 37 (2011) 1589–1594.
- M. Dogan, A. Harun, A. Mahir, Adsorption of methylene blue onto hazelnut shell: Kinetics, mechanism and activation parameters, *J. Hazard. Mater.* doi: 10.1016/j.jhazmat.2008.07.155
- I.M. Robinson, G. McMullan, R. Marchant, P. Nigam, Remediation of dyes in textile effluent: A critical review on current treatment technologies, *Bioresour. Technol.* 77 (2001) 247–255.
- Z. Aksu, S. Tezer, Equilibrium and kinetic modeling of biosorption of Remazol Black B by *Rhizopus arrhizus* in a batch system: Effect of temperature, *Process Biochem.* 36 (2000) 431–439.
- T. Robinson, B. Chandran, P. Nigam, Removal of dyes from artificial textile dye effluent by two agricultural waste residues, corncob and barley husk, *Environ. Int.* 28 (2002) 29–33.
- Z. Aksu, Application of biosorption for the removal of organic pollutants: A review, *Process Biochem.* 40 (2005) 997–1026.
- E.A. Clarke, R. Anliker, Organic dyes and pigments, *Handbook of Environmental Chemistry, Anthropogenic Compounds.* 3A (1980) 181–215
- G. Mishra, M.A. Tripathy, A critical review of the treatment for decolorization of textile effluent, *Colourage* 40 (1993) 35–38.
- R. Han, D. Ding, Y. Xu, W. Zou, Y. Wang, Y. Li, L. Zou, Use of rice husk for adsorption of Congo red from aqueous solution in column mode, *Bioresour. Technol.* 99 (2008) 2938–2946.
- P. Senthil Kumar, S. Ramalingam, C. Senthamarai, M. Niranjana, P. Vijayalakshmi, S. Sivanesan, Adsorption of dye from aqueous solution by cashew nut shell: Studies on equilibrium isotherm, kinetics and thermodynamics of interactions, *Desalination* 261 (2010) 52–60.
- M. Rafatullah, O. Sulaiman, R. Hashim, A. Ahmad, Adsorption of methylene blue on low-cost adsorbents: A review, *J. Hazard. Mater.* 177 (2010) 70–80.
- S. Chowdhury, S. Chakraborty, P. Saha, Biosorption of basic green 4 from aqueous solution by *Ananas comosus* (pineapple) leaf powder, *Colloids Surf. B: Biointer.* 84 (2011) 520–527.
- M.S. El-Geundi, Colour removal from textile effluents by adsorption techniques, *Water Res.* 25 (1991) 271–273.
- A.E. Ofomaja, Y.S. Ho, Equilibrium sorption of anionic dye from aqueous solution by palm kernel fibre as sorbent, *Dyes Pigm.* 74 (2007) 60–66.
- S. Chowdhury, R. Mishra, P. Saha, P. Kushwaha, Adsorption thermodynamics, kinetics and isosteric heat of adsorption of malachite green onto chemically modified rice husk, *Desalination* 265 (2011) 159–168.
- R. Malik, D.S. Ramteke, S.R. Wate, Adsorption of malachite green on groundnut shell waste based powdered activated carbon, *Waste Manage.* 27(9) (2007) 1129–1138.
- K.V. Kumar, K. Porkodi, Batch adsorber design for different solution volume/adsorbent mass ratios using the experimental equilibrium data with fixed solution volume/adsorbent mass ratio of malachite green onto orange peel, *Dye Pigm.* 74 (2007) 590–594.
- K.V. Kumar, Optimum sorption isotherm by linear and non-linear methods for malachite green onto lemon peel, *Dye Pigm.* 74 (2007) 595–597.
- X.S. Wang, Y. Zhou, Y. Jiang, C. Sun, The removal of basic dyes from aqueous solutions using agricultural by-products, *J. Hazard. Mater.* 157 (2008) 374–385.
- S. Preethi, A. Sivasamy, Removal of safranin basic dye from aqueous solutions by adsorption onto corncob activated carbon, *Ind. Eng. Chem. Res.* 45 (2006) 7627–7632.
- P.D. Saha, S. Chakraborty, S. Chowdhury, Batch and continuous (fixed-bed column) biosorption of Crystal Violet by *Artocarpus heterophyllus* (jackfruit) leaf powder, *Colloids Surf. B: Biointer.* 92 (2012) 262–270.
- S. Chowdhury, R. Mishra, P. Kushwaha, P. Das, Optimum sorption isotherm by linear and non-linear methods for safranin onto alkali treated rice husk, *Bioremed. J.* 15 (2011) 77–89.
- T.W. Weber, R.K. Chakkravorti, Pore and solid diffusion models for fixed-bed adsorbents, *J. AIChE* 20 (1974) 228–238.
- E. Bulut, M. Ozacar, Adsorption of malachite green onto bentonite: Equilibrium and kinetic study and process design, *Micropor. Mesopor. Mater.* 115 (2008) 234–246.
- S. Karagoz, T. Tay, S. Ucar, Activated carbon from waste biomass by sulphuric acid activation and their use on methylene blue adsorption, *Bioresour. Technol.* 99 (2008) 6214–6222.
- A.A. Poghossian, Determination of the pH_{zpc} of insulators surface from capacitance—voltage characteristics of MIS and EIS structures, *Sens. Actuat. B: Chem.* 44 (1997) 551.

- [29] S. Nethaji, A. Sivasamy, G. Thennarasu, S. Saravanan, Adsorption of Malachite Green dye onto activated carbon derived from *Borassus aethiopicum* flower biomass, *J. Hazard. Mater.* 181 (2010) 271–280.
- [30] M.T. Uddin, M. Rukanuzzaman, M.M.R. Khan, M.A. Islam, Adsorption of methylene blue from aqueous solution by jackfruit (*Artocarpus heterophyllus*) leaf powder: A fixed-bed column study, *J. Environ. Manage.* 90 (2009) 3443–3450.
- [31] S. Chowdhury, S. Chakraborty, P. Saha, Biosorption of basic green 4 from aqueous solution by *Ananas comosus* (pineapple) leaf powder, *Colloids Surf. B: Biointer.* 84 (2011) 520–527.
- [32] P. Kumari, P. Sharma, M.M. Srivastava, Biosorption studies on shelled moringa oleifera lamarck seed powder: Removal and recovery of arsenic from aqueous system, *Int. J. Miner. Process.* 78 (2006) 131–139.
- [33] M. Yurtsever, I.A. Sengil, Biosorption of Pb (II) ions by modified quebracho tannin resin, *J. Hazard. Mater.* 163 (2009) 58–64.
- [34] R. Kumar, R. Ahmad, Biosorption of hazardous crystal violet dye from aqueous solution onto treated ginger waste (TGW), *Desalination* 265 (2011) 112–118.
- [35] S. Chakraborty, S. Chowdhury, P.D. Saha, Adsorption of crystal violet from aqueous solution onto NaOH-modified rice husk, *Carbohydr. Poly.* 86 (2011) 1533–1541.
- [36] R. Ahmad, Studies on adsorption of crystal violet dye from aqueous solution onto coniferous pinus bark powder (CPBP), *J. Hazard. Mater.* 171 (2009) 767–773.
- [37] A. Saeed, M. Sharif, M. Iqbal, Application potential of grapefruit peel as dye sorbent: Kinetic, equilibrium and mechanism of crystal violet adsorption, *J. Hazard. Mater.* 179 (2010) 564–572.
- [38] O. Aksakal, H. Ucun, Equilibrium, kinetic and thermodynamic studies of the biosorption of textile dye (reactive red 195) onto *Pinus sylvestris* L., *J. Hazard. Mater.* 181 (2010) 666–672.
- [39] G. Crini, H.N. Peindy, F. Gimbert, C. Robert, Removal of C. I. Basic green4 (Malachite Green) from aqueous solution by adsorption using cyclodextrin-based adsorbent: Kinetic and equilibrium studies, *Sep. Purif. Technol.* 53 (2007) 97–110.
- [40] E. Eren, O. Cubuk, H. Ciftci, B. Eren, B. Caglar, Adsorption of basic dye from aqueous solution by modified sepiolite: Equilibrium, kinetic and thermodynamic study, *Desalination* 252 (2010) 88–96.
- [41] C. Namasivayam, M.D. Kumar, K. Selvi, R.A. Begum, T. Vanathi, R.T. Yamuna, Waste' coir pith – A potential biomass for the treatment of dyeing wastewaters, *Biomass Bioenergy.* 6 (2001) 477–483.
- [42] S.D. Khattri, M.K. Singh, Colour removal from dye wastewater using sugar cane dust as an adsorbent, *Adsorp. Sci. Technol.* 17 (1999) 269–282.
- [43] S.D. Khattri, M.K. Singh, Color removal from *synthetic dye* wastewater using a bioadsorbent, *Water Air Soil Pollut.* 120 (2000) 283–294.
- [44] H. Ali, S.K. Muhammad, Biosorption of crystal violet from water on leaf biomass of *Calotropis procera*, *J. Environ. Sci. Technol.* 1 (2008) 143–150.
- [45] S.D. Khattri, M.K. Singh, Use of sagaun sawdust as an adsorbent for the removal of crystal violet dye from simulated wastewater, *Environ. Prog. Sustainable Energy* 31(3) (2012) 435–442.
- [46] H. Parab, M. Sudersanan, N. Shenoy, T. Pathare, B. Vaze, Use of agro-industrial wastes for removal of basic dyes from aqueous solutions, *Clean: Soil Air Water* 37 (2009) 963–969.
- [47] K.S. Bharathi, S.T. Ramesh, Equilibrium, thermodynamic and kinetic studies on adsorption of a basic dye by *Citrullus lanatus* rind, *Iranica J. Energy Environ.* 3(1) (2012) 23–34.
- [48] G. Annadurai, R.S. Juang, D.-J. Lee, Use of cellulose-based wastes for adsorption of dyes from aqueous solutions, *J. Hazard. Mater.* 92 (2004) 263–274.
- [49] S. Jain, R.V. Jayaram, Removal of basic dyes from aqueous solution by lowcost adsorbent: Wood apple shell (*Feronia acidissima*), *Desalination* 250 (2010) 921–927.
- [50] K. Porkodi, K.V. Kumar, Equilibrium, kinetics and mechanism modeling and simulation of basic and acid dyes sorption onto jute fiber carbon: Eosin yellow, malachite green and crystal violet single component systems, *J. Hazard. Mater.* 143 (2007) 311–327.
- [51] X.S. Gupta, Suhas Application of low-cost adsorbents for dye removal—A review, *J. Environ. Manage.* 90 (2009) 2313–2342.
- [52] X.S. Wang, X. Liu, L. Wen, Y. Zhou, Y. Jiang, Z. Li, Comparison of basic dye crystal violet removal from aqueous solution by low-cost biosorbents, *SEPA, Sep. Sci. Technol.* 43 (2008) 3712–3731.